

## **Predictive Functional Control of Superheat in a Refrigeration System using a Neural Network Model**

Pedersen, Tom Søndergård; Nielsen, Kirsten Mølgaard; Hindsborg, Jeff ; Reichwald, Peter; Vinther, Kasper; Izadi-Zamanabadi, Roozbeh

*Published in:*  
IFAC-PapersOnLine

*DOI (link to publication from Publisher):*  
[10.1016/j.ifacol.2017.08.008](https://doi.org/10.1016/j.ifacol.2017.08.008)

*Publication date:*  
2017

*Document Version*  
Publisher's PDF, also known as Version of record

[Link to publication from Aalborg University](#)

*Citation for published version (APA):*  
Pedersen, T. S., Nielsen, K. M., Hindsborg, J., Reichwald, P., Vinther, K., & Izadi-Zamanabadi, R. (2017). Predictive Functional Control of Superheat in a Refrigeration System using a Neural Network Model. *IFAC-PapersOnLine*, 50(1), 43-48. <https://doi.org/10.1016/j.ifacol.2017.08.008>

### **General rights**

Copyright and moral rights for the publications made accessible in the public portal are retained by the authors and/or other copyright owners and it is a condition of accessing publications that users recognise and abide by the legal requirements associated with these rights.

- Users may download and print one copy of any publication from the public portal for the purpose of private study or research.
- You may not further distribute the material or use it for any profit-making activity or commercial gain
- You may freely distribute the URL identifying the publication in the public portal -

### **Take down policy**

If you believe that this document breaches copyright please contact us at [vbn@aub.aau.dk](mailto:vbn@aub.aau.dk) providing details, and we will remove access to the work immediately and investigate your claim.



# Predictive Functional Control of Superheat in a Refrigeration System using a Neural Network Model

T.S. Pedersen\* K.M. Nielsen\* J. Hindsborg\* P. Reichwald\*  
 K. Vinther\* R. Izadi-Zamanabadi\*\*

\* *Institute of Electronic Systems, Automation and Control, Aalborg University, Aalborg, Denmark (e-mail: tom, kmn, kv@es.aau.dk).*

\*\* *At Aalborg University and also at Danfoss A/S Electronic Controllers and Services, Nordborg, Denmark (e-mail: roozbeh@danfoss.com)*

**Abstract:** This paper compares three methods for control of the superheat in a refrigeration system. A traditional gain scheduled PI-based controller, a predictive functional controller (PFC) and a predictive functional controller with a neural network model (PFCNN). The aim is to investigate the performance of the three controllers with respect to disturbance rejection measured both at the superheat deviation from the reference and the actuation of the expansion valve. The controllers are designed and tested on a laboratory set-up. The performance of the controllers turns out to be similar and distinguish between the concepts must be based on other parameters like tuning and demands for computational power.

© 2017, IFAC (International Federation of Automatic Control) Hosting by Elsevier Ltd. All rights reserved.

**Keywords:** Refrigeration system control, Predictive control, Neural networks, PID control.

## 1. INTRODUCTION

Refrigeration systems are widely used and among the most electrical energy consuming equipment in supermarkets. Refrigeration systems normally contain a refrigerant operating continuously between vaporization and compression. This process is implemented by a valve, an evaporator, a compressor and a condenser, and this set-up remains to a considerable extent the same in most refrigeration systems. The details of the vapour compression type refrigeration process are not given here, but can be found in e.g. Vinther (2013).

Larger refrigeration systems are normally controlled by three SISO PI-controllers. One is controlling the compressor to achieve an appropriate pressure in the evaporator ensuring a suitable saturation temperature. The condenser fan velocity is similarly PI controlled to ensure a certain condensation temperature. Finally the superheat is controlled using the opening degree (OD) of the expansion valve. The control of the superheat is in focus in this work. Different control concepts has been investigated in Vinther (2013), Rasmussen et al. (2009), Elliott et al. (2010), Vinther et al. (2013) and Vinther et al. (2012).

Super-heating of the refrigerant beyond the evaporation temperature is important, since no superheat means that two-phase refrigerant will enter the compressor and increase the power consumption and wear. This means that the flow through the valve must be kept at a level, where all the refrigerant is evaporated before it reaches the compressor. At the same time, it is important to have as much two-phase refrigerant in the evaporator as possible, to increase the heat transfer and thus optimize the refrigeration process.

So a key variable, which greatly affects the efficiency of a refrigeration system, is the superheat, which again is an indirect measure of the filling of the evaporator. Normally the superheat is measured using the saturation pressure in the evaporator and the outlet vapour temperature at the evaporator output; these are combined to give the superheat. In our work we will compare three different controllers namely a gain scheduled PI controller, a predictive functional controller (PFC) and a neural network based PFC. PFC has been investigated for superheat control in Changenet et al. (2008) and Fallahsohi et al. (2009), with promising results. PFC with a neural network model has been suggested for highly non-linear systems, Yang et al. (2005) and Guo (2006); the present system is non-linear especially in the small signal gain, which could justify adding a neural network model to PFC. The control concepts are tested on a full scale laboratory set-up.

Most refrigeration systems are equipped with computers not suited for large computational tasks. The gain scheduled PI controller and the PFC with fixed difference equation model demands few computations. A trained neural network will not increase the computational effort considerably, but the training of a neural network constitutes a computational problem and must be done prior to commissioning.

Section 2 describes the laboratory set-up. The modelling of the expansion valve and the evaporator is presented in Section 3. Section 4 explains the control strategies and controller adjustments, Section 5 provides a comparison of the three control concepts and concluding remarks are finally given in Section 6.

## 2. DESCRIPTION OF THE TEST SET-UP

A refrigeration system with full scale components is available at Aalborg University. A simplified schematic of the test set-up is presented in Fig. 1. This system has an

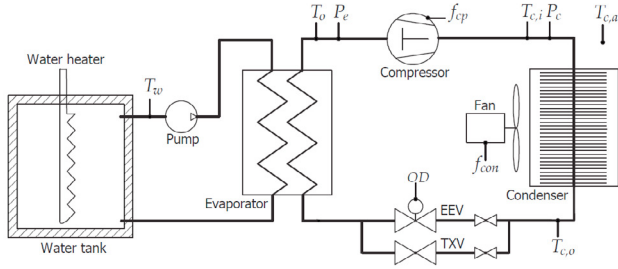


Fig. 1. Refrigeration laboratory system test set-up (a water chiller system), Vinther (2013).

approximate maximum cooling capacity of 4 kW and water is circulated on the secondary side of the evaporator in a circuit with a 60 litre water tank, a pump, and a heater. The refrigerant is R134a and the system also consists of a scroll compressor, a condenser unit, and interchangeable expansion valves; this can be either a stepper motor, EEV, or a thermostatic expansion valve, TEV. It is possible to control the OD of the EEV valve. The power to the water heater is controllable and can be seen as a disturbance to the system. The condenser pressure is controlled using the frequency of the condenser fan ensuring a reference pressure. The suction pressure  $P_e$  is controlled using the scroll compressor frequency. Sensors measuring temperatures and pressures, with a sampling interval of 1 second, are indicated in the figure. A more detailed description of the set-up can be found in Vinther (2013).

## 3. MODELLING OF SUPERHEAT

The evaporator superheat control set-up in focus is illustrated in Fig. 2. Pressure  $P_e$  and the outlet temperature  $T_o$  from the evaporator are measured. The pressure  $P_e$  is converted to the corresponding saturation temperature  $T_e$ ; this is subtracted from  $T_o$  giving the superheat temperature  $T_{sh}$ .

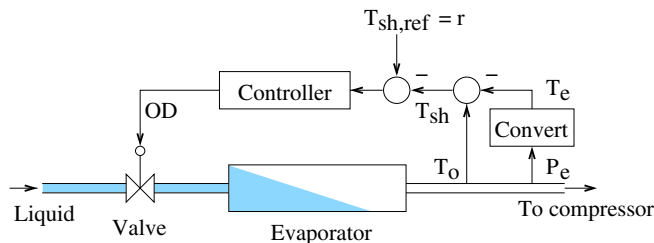


Fig. 2. Control of the superheat using the valve OD.

A small signal model from the valve OD to the superheat can be described by a first order system with delay, Vinther (2013), Rasmussen et al. (2009), Vinther et al. (2013)

$$\hat{T}_{sh}(s) = \frac{K}{\tau s + 1} e^{-T_d s} \hat{OD}(s), \quad (1)$$

where  $\hat{\cdot}$  indicates small signal values,  $K$  is the small signal gain,  $\tau$  is a time constant and finally  $T_d$  is a time delay.

The small signal gain can be found from an experiment, see Fig. 3. In the experiment OD is slowly increased from 40.5% to 43.2%. The absolute value of the superheat is measured and is going from 15°C to 2°C; the small signal gain is the slope of this curve and can be found by making an approximation to the absolute superheat followed by finding the derivative of the approximation.

A potential approximation of the curve  $T_{sh}$  as function of OD is Vinther (2013)

$$T_{sh} \approx -k_1 \arctan(k_2(OD - \bar{OD})) + \bar{T}_{sh}, \quad k_1, k_2 > 0, \quad (2)$$

where bar's are offsets and  $k_1, k_2$  are parameters. The four parameters are fitted to the graph and plotted in Fig. 3. The small signal gain is now found as

$$K = \frac{dT_{sh}}{dOD} = -\frac{k_1 k_2}{1 + (k_2(OD - \bar{OD}))^2}, \quad (3)$$

which is also shown in Fig. 3 along with a simple numerical derivation.

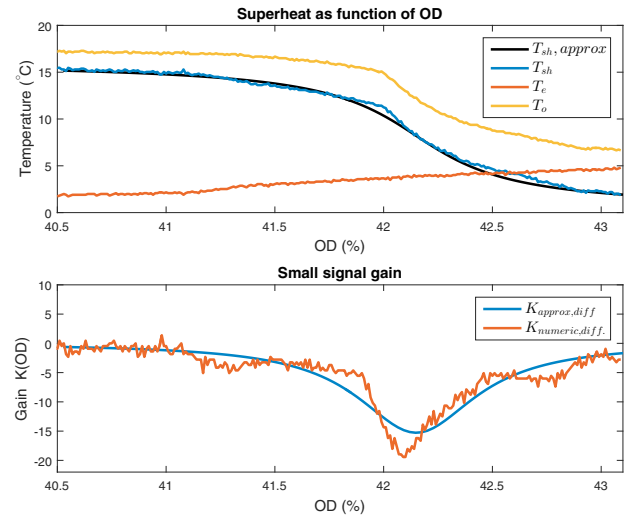


Fig. 3. Measured superheat as function of OD (upper plot). Small signal gain (lower plot).

It is seen in Fig. 3 that the gain  $K$  is very dependent of the OD value. For varying outdoor temperatures,  $T_{air,o}$ , or water heater powers, the cooling capacity is changed, meaning that the OD has a different operating point given as the center point in the *atan* function. Measurements indicate that shape of the *atan* function is the same for all center points giving the same small signal gain profile.

To overcome the variations caused by changing cooling capacity it is appropriate to have integral action in the controller. The variations in small signal gain can either be solved by gain scheduling or alternatively by use of a neural network.

## 4. CONTROL CONCEPTS

The aim of the superheat control is to maintain a constant (and low) superheat. In larger refrigeration systems the superheat is controlled using a standard PI controller, this will be the underlying basis for benchmarking the controllers. The two other controllers have their point of origin in predictive functional control (PFC) where the first is based on Richalet et al. (2014) and Richalet et al.

(2011); a first order system with delay is used as model for calculating the control response. The third controller broadens the PFC using a radial basis function neural network (RBFNN) as model instead of the linear first order system, Yang et al. (2005), Guo (2006).

The PI controller is on the form

$$OD(s) = (-K_p - K_i \frac{1}{s})E(s), \quad (4)$$

where  $OD(s)$  is control output,  $E(s)$  is control input and  $K_p, K_i$  are PI coefficients. Standard anti-integrator wind-up is included. To deal with the system gain non-linearity the PI controller gain is gain-scheduled using three operating points and by making a linear interpolation between the points.

In PFC the idea is to calculate a constant controller output that, within a given time horizon, will reduce the control error by a certain factor.

The control error  $e$  must be reduced according to

$$e(n+h) = e(n)\lambda^h, \quad (5)$$

where  $\lambda < 1$  is a constant,  $h$  is the time horizon or the desired coincidence point, meaning that the error will be reduced with the factor  $\lambda^h$ . According to Fig. 4

$$\begin{aligned} e(n) &= \Delta p + e(n+h) = \Delta p + e(n)\lambda^h \Rightarrow \\ \Delta p &= (1 - \lambda^h)e(n) = (1 - \lambda^h)(r - T_{sh}(n)), \end{aligned} \quad (6)$$

where  $\Delta p$  is the desired change of the process output from time  $n$  to time  $n+h$ . The controller task is to find an  $OD$  signal, which is constant from  $n$  to  $n+h$ , such that the process output is changed by  $\Delta p$ .

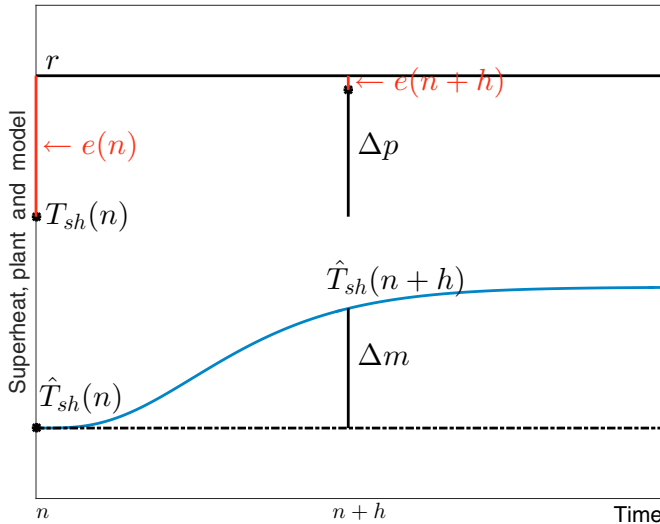


Fig. 4. Illustration of PFC functionality.

The discrete version of the first order model with delay given in (1) is

$$\hat{T}_{sh}(n+1) = a\hat{T}_{sh}(n) + K(1-a)\hat{OD}(n-q), \quad (7)$$

where  $a = e^{-T_s/\tau}$ ,  $T_s$  is the sampling time, and  $qT_s = T_d$ . Given a constant input, the output of the model is given as

$$\hat{T}_{sh}(n+h) = a^h\hat{T}_{sh}(n) + K(1-a^h)\hat{OD}(n-q). \quad (8)$$

If we want the output of the model to change  $\Delta m = \Delta p$ , from time  $n$  to  $n+h$ , then

$$\Delta p = \hat{T}_{sh}(n+h) - \hat{T}_{sh}(n). \quad (9)$$

Inserting  $\hat{T}_{sh}(n+h)$  gives

$$\Delta p = (a^h - 1)\hat{T}_{sh}(n) + K(1-a^h)\hat{OD}(n-q). \quad (10)$$

Solving this equation for  $\hat{OD}(n-q)$  gives

$$\hat{OD}(n-q) = \frac{\Delta p}{K(1-a^h)} + \frac{1}{K}\hat{T}_{sh}(n), \quad (11)$$

$$= \frac{1-\lambda^h}{K(1-a^h)}(r - T_{sh}(n)) + \frac{1}{K}\hat{T}_{sh}(n). \quad (12)$$

Because we want to find  $\hat{OD}(n)$  the equation is time shifted

$$\hat{OD}(n) = \frac{1-\lambda^h}{K(1-a^h)}(r - T_{sh}(n+q)) + \frac{1}{K}\hat{T}_{sh}(n+q). \quad (13)$$

The last term is not problematic because  $\hat{T}_{sh}(n+q)$  is calculated from the time shifted version of (1)

$$\hat{T}_{sh}(n+q) = a\hat{T}_{sh}(n+q-1) + K(1-a)\hat{OD}(n-1); \quad (14)$$

a term that can be calculated at the previous sample time. The term  $T_{sh}(n+q)$  is estimated from

$$T_{sh}(n+q) - T_{sh}(n) = \hat{T}_{sh}(n+q) - \hat{T}_{sh}(n), \quad (15)$$

giving the estimate

$$T_{sh}^*(n+q) = T_{sh}(n) + \hat{T}_{sh}(n+q) - \hat{T}_{sh}(n). \quad (16)$$

Inserting (16) in (13), the final algorithm is

$$\hat{OD}(n) = \frac{1-\lambda^h}{K(1-a^h)}(r - T_{sh}^*(n+q)) + \frac{1}{K}\hat{T}_{sh}(n+q). \quad (17)$$

Equation (14) and (16) are updated for each sample.

Even though there is no integrator in the control algorithm, the steady state error will be zero, see Richalet et al. (2011). If the system is stable the steady state gain of the model is

$$\hat{T}_{sh,ss} = K\hat{OD}_{ss} \Rightarrow \hat{OD}_{ss} = \frac{1}{K}\hat{T}_{sh,ss}. \quad (18)$$

Inserting this in control algorithm (17) gives

$$\begin{aligned} \frac{1}{K}\hat{T}_{sh,ss} &= \frac{1-\lambda^h}{K(1-a^h)}(r - T_{sh,ss}) + \frac{1}{K}\hat{T}_{sh,ss} \\ \Rightarrow r - T_{sh,ss} &= 0, \end{aligned} \quad (19)$$

resulting in no steady state error, as it is the case for a PI-controller.

The structure of the PFC can be seen in the upper part of Fig. 5. Due to the non-linearities in the plant as indicated in Fig. 3, the linear model may not be an appropriate way to predict the correct plant output at time  $n+h$ . Therefore a more accurate model is desirable. Measurements from the laboratory test set-up gives a unique opportunity to construct a data driven model; neural networks offers a possibility to include measurements in an intelligent manner. The linear model is therefore replaced by a neural network model in the lower part of Fig. 5. The neural network is both used by the PFC and by a solver, which iteratively searches for an  $\hat{OD}_s$  that gives the desired  $\Delta p$  at time  $n+h$ .

In Park et al. (1991) it has been proven that a Radial Basis Function Neural Network (RBFNN), see Fig. 6, has universal approximation capability for a non-linear function assuming only one hidden layer.

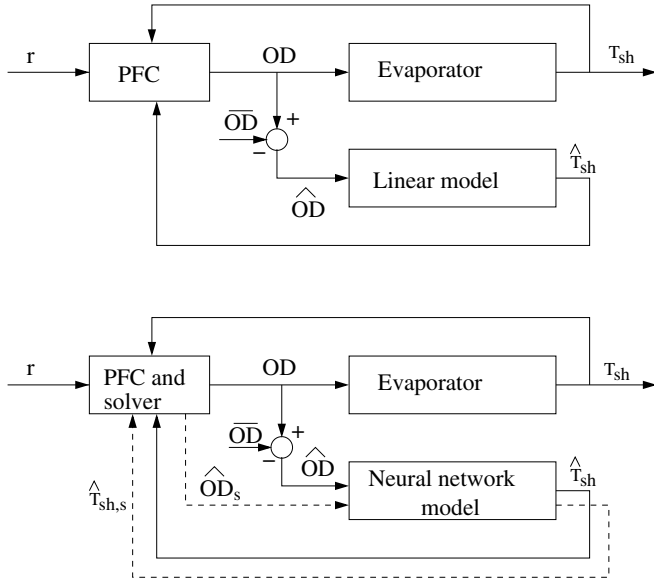


Fig. 5. The structure of PFC with and without NN.

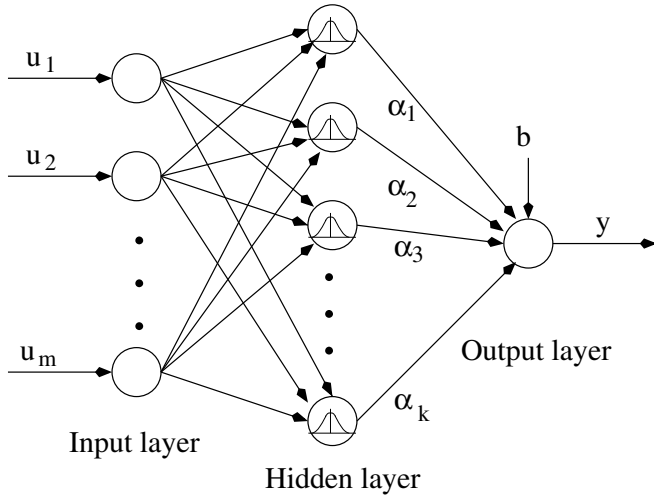


Fig. 6. The structure of a RBF neural network.

The overall network output is

$$y(\mathbf{u}) = \mathbf{b} + \sum_{i=1}^k \alpha_i f_i(\mathbf{u}) \quad (20)$$

and

$$f_i(\mathbf{u}) = \exp\left(-\frac{1}{\sigma_i^2} \|\mathbf{u} - \mu_i\|^2\right), \quad (21)$$

where  $b$  is an offset,  $\alpha$  are weight factors from the hidden layer to the output,  $f_i$  are neuron functions dependent on the center  $\mu_i$  and the width,  $\sigma_i$ , of the radial basis function. In training, which is based on back-propagation learning, the parameters  $\mu, \sigma, \alpha, b$  are adjusted to fit a measured data-set.

Modelling of dynamic systems using neural networks can be performed in different ways, Bhushan et al. (2011). To include the dynamics of the process, the RBFNN is extended with time delays, making it possible to cope with difference equations, see Fig. 7.

The number of neurons and connections have been determined by splitting the data set into two parts, one for

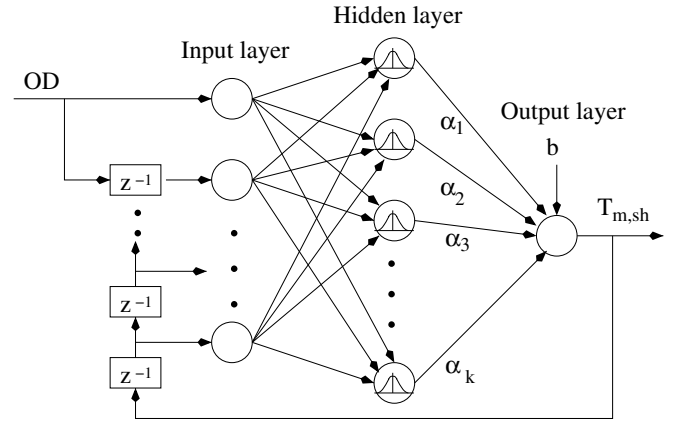


Fig. 7. The structure of RBF neural network for a SISO dynamic system.

training and one for verification. The model output from the neural network is simple to calculate, but a problem using a neural network in the PFC is to determine which constant value of  $\hat{OD}$  gives a certain  $\Delta p$ . For the linear model this is simply found by using (11), in the neural network case a search algorithm for finding the desired value of  $OD$  must be used, this complicates the neural network solution. The neural network solution is shown in the lower part of Fig. 5 where the neural network model is used twofold, it is a simulation model where it calculates  $\hat{T}_{sh}(n)$ , but is also used to forecast the value  $\hat{T}_{sh}(n+h)$  to calculate  $\hat{OD}_s$ .

## 5. TEST RESULTS

The three controllers mentioned have been tested on the laboratory set-up and all the results can be found in Hindsborg et al. (2016). A disturbance sequence, as shown in the top of Fig. 8, containing variations in compressor frequency and power to the water heater, is applied to the system. The sequence is constructed to include nearly steady state conditions, shifts in disturbance signals individually and simultaneously, in this way the systems are tested. It is chosen to use a superheat reference  $T_{sh,ref} = 8^\circ\text{C}$  to avoiding liquid entering the compressor, though in Vinther (2013) this value results in oscillatory output (also when using a TEV), because the system gain is very high in this operating point. However, detuning the controllers would result in too slow disturbance rejection (risk of flooding).

The PI controller parameters  $K_i, K_p$  are tuned to three operating points according to the different small signal gains as shown in Fig. 3 and gain-scheduled using linear interpolation.

In the PFC prediction model, the parameters  $K, \tau, T_d$  are determined using system identification in a typical operating point as described in Section 3, see also Vinther (2013); Hindsborg et al. (2016). For the prediction horizon  $h$  a short (15 s), medium (30 s), and long (45 s) have been examined; the chosen value 30 s is a compromise between fast response and low noise sensitivity. The damping factor  $\lambda^h$  is set to 0.05.

In the PFC with neural network model, the RBFNN structure must be determined. Candidates of the RBFNN with different numbers of neurons, number of delayed

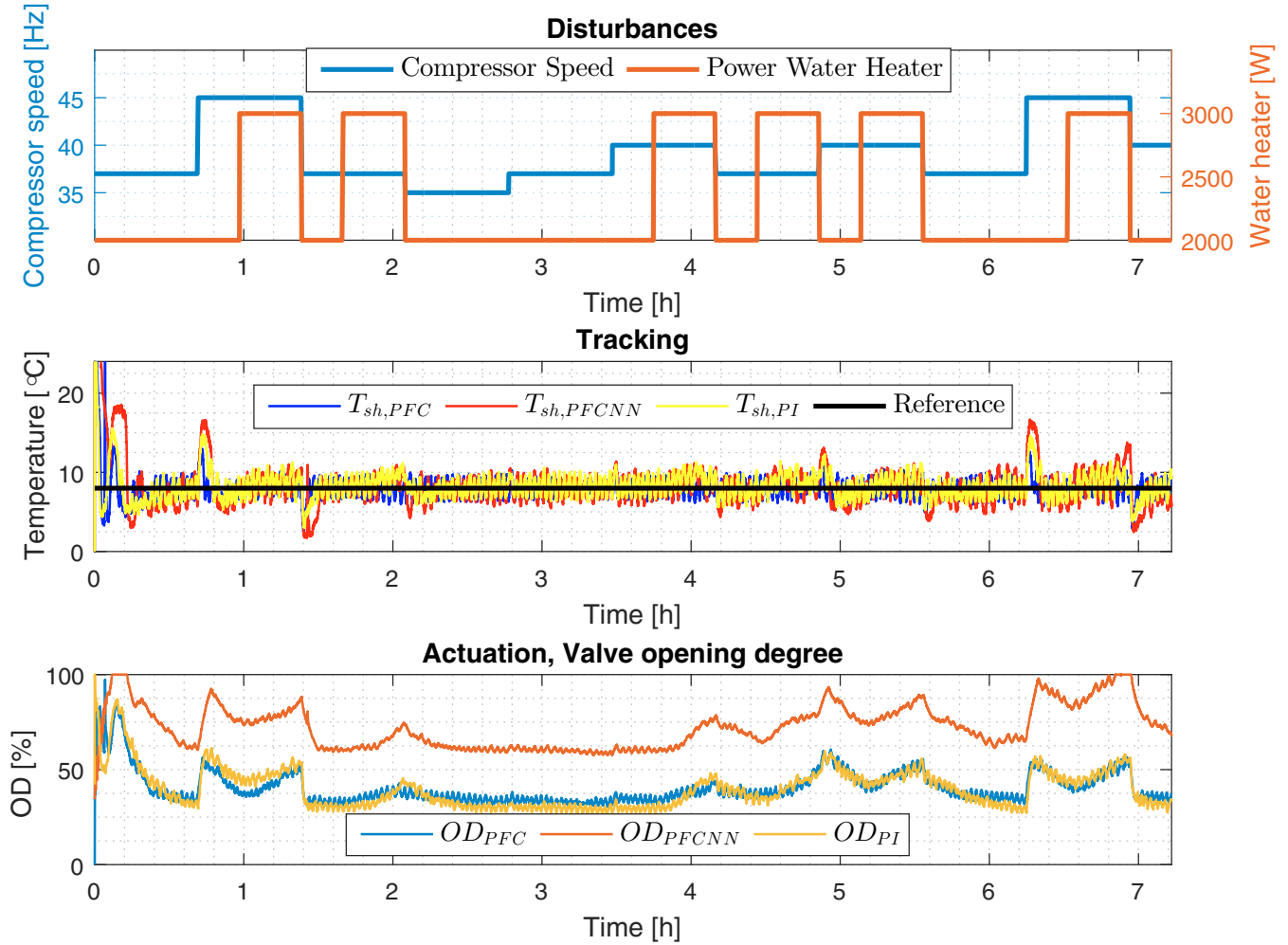


Fig. 8. The disturbance sequence given by compressor speed and power to the water heater.

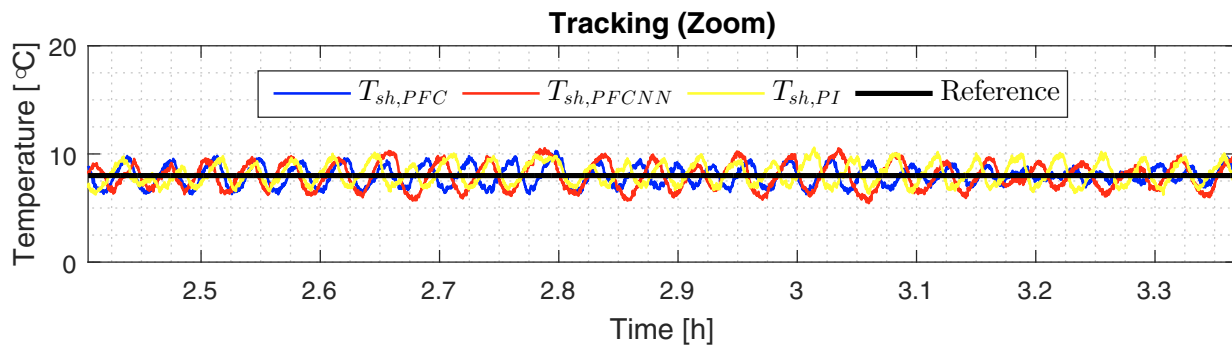


Fig. 9. A zoom on the superheat plot during the disturbance sequence given by compressor speed and power to the water heater.

inputs and number of delayed output have been trained using a training data set. The candidates have been compared using an evaluation data set. RBFNN is used to determine which constant input  $OD(n)$  must be used in order to obtain a change  $\Delta m = \Delta p$  (see (6)) at time  $n+h$ ; this cannot be solved analytically therefore a numerical solver is used.

In Fig. 8 the three controllers have been tested using the disturbance sequence and the reference  $T_{sh,ref} = 8^\circ\text{C}$ .

Seemingly all three controllers give responses with no steady state errors. Disturbances on either compressor speed or water heater power solely implies only small superheat variations. Simultaneously load changes introduce larger deviations from the set-point but still in an acceptable range; the superheat do not reach zero. Due to steady state behaviour it is difficult to distinguish between the controllers. Shifts in one disturbance don't give large superheat variations. The most problematic is when both compressor speed and water heater power are shifted

simultaneously as at approx. 2.1, 4.2, 4.8 and 6.9 hours; here the PFC performs better than the PI controller and the PFCNN causes large output variations. In Fig. 9 is a zoom of the superheat variations. Here it is seen that at steady state the three controllers acts very similar.

In Fig. 8 the lower plot shows the actuation, these are similar and the variations correspond to the disturbances. As seen the valve-opening is larger for the PFCNN controller than the other controller, this is caused by a large difference in the ambient temperature (the experiments were performed at different weather conditions in the spring).

All in all the performance of the three controllers are quite similar. This implies that the choice of controller is more a question of tuning and implementation than of performance. Unfortunately the test-bench is constructed so the set-point used for the superheat gives sinusoidal variations making it difficult to compare the results of the controllers. PFCNN requires large amount of training data and demands storage and computational capacity of the control computer. The two other candidates are less demanding. One advantage of the PFC is the ability to remove the steady state error without an integrator, a disadvantages is that the PFC operates on a small signal data. The PI controller can operate on absolute signals but an anti-integrator wind-up algorithm is a must.

## 6. CONCLUSION

In the paper three different control strategies for control of the superheat in a refrigeration system have been introduced. The three strategies are gain scheduled PI control, predictive functional control and finally predictive functional control using neural network. The controllers are tested in a laboratory set-up using real refrigeration components. The performance is similar implying that the choice of control strategy can be motivated by other parameters like tunability and demands for computational capacity.

## REFERENCES

- B. Bhushan, M. Singh and A. Hage. Identification and control using MLP, Elman, NARXSP and radial basis function networks: a comparative analysis. *Springer Science+Business Media B.V.*, 2011
- C. Changelnet, J.N. Charvet, D. Gehin, F. Sicard and B. Chamel. Study on predictive functional control of an expansion valve for controlling the evaporator superheat. *Proc. IMechE Vol 222, Part I, Systems and Control Engineering*, 28 may 2008.
- M. S. Elliott and B. P. Rasmussen. On reducing evaporator superheat nonlinearity with control architecture. *International Journal of Refrigeration* 33(3), 607–614. 2010.
- H. Fallahsohi, C. Changelnet, S. Place, C. Ligeret and X. Lin-Shi d. Predictive functional control of an expansion valve for minimizing the superheat of an evaporator. *International Journal of Refrigeration* 3, 409 – 418, 2009.
- J. Hindsborg and Peter Reichwald. Control of Refrigeration Systems – A Comparative Study. *Master thesis*. Aalborg University, Denmark, June 2016.
- J. Park and I. W. Sandberg. Universal Approximation Using Radial-Basis-Function Networks. *Neural Computation*, Vol. 3, No. 2, Pages 246–257, 1991.
- Peng Guo. Nonlinear Predictive Functional Control based on Hopfield Network and its application in CSTR. *Proc. of the Fifth International Conference on Machine Learning and Cybernetics*, Dalian, 13-16, August 2006
- H. Rasmussen and L. F. S. Larsen. Nonlinear superheat and capacity control of a refrigeration plant. *Mediterranean Conference on Control & Automation* (pp. 1072–1077). Thessaloniki, Greece. 2009.
- J. Richalet and D. O'Donovan. Elementary Predictive Functional Control: A Tutorial. *Proc. Advanced Control of Industrial Processes*, Thousand Islands Lake, Hangzhou, China May 2-26, 2011.
- J. Richalet, T. Darure and J. Mallet. Predictive Functional Control of counter current heat exchangers. *19th World Congress. The International Federation of Automatic Control*, Cape Town, South Africa. August 24-29, 2014.
- K. Vinther. Data-Driven Control of Refrigeration Systems *PhD thesis*, Aalborg University, Denmark, November 2013.
- K. Vinther, H. Rasmussen, R. Izadi-Zamanabadi, and J. Stoustrup. Single temperaturesensor superheat control using a novel maximum slope-seeking method. *International Journal of Refrigeration* vol. 36, issue 3, pp. 1118–1129, 2013.
- K. Vinther, C. H. Lyhne, E. B. Sørensen, and H. Rasmussen. Evaporator Superheat Control with One Temperature Sensor using Qualitative System Knowledge. *American Control Conference*, Montreal, Canada, pp. 374–379, June 2012.
- X. Yang, D. Xu, X. Han and H. Zhou. Predictive Functional Control with Modified Elman Neural Network for Reheated Steam Temperature. *Proc. of 4'th International Conference on Machine Learning and Cybernetics*, Guangzhou, 18-21 August 2005.